International Journal of Thermophysics, Vol. 26, No. 6, November 2005 (© 2005)
DOI: 10.1007/s10765-005-8596-1

Supercooling Water in Cylindrical Capsules[1]

J. J. Milón Guzman[2] and S. L. Braga[3,4]

An experimental apparatus was developed to investigate the supercooling phenomenon of water inside cylindrical capsules used for a cold storage process. The coolant is a water–alcohol mixture controlled by a constant temperature bath (CTB). Temperatures varying with time are measured inside and outside the capsule. Cylinders with an internal diameter and thickness of 45 and 1.5 mm, respectively, were made from four different materials: acrylic, PVC, brass, and aluminum. The supercooling period of the water and the nucleation temperature were investigated for different coolant temperatures. The supercooling and nucleation probabilities are shown as a function of the coolant temperature for the four different materials.

KEY WORDS: air conditioning; nucleation; phase change; refrigeration; supercooling; thermal storage.

1. INTRODUCTION

Thermal storage for refrigeration systems is an important concept of many energy conservation programs. Water is widely used as the phase-change material (PCM) due to its advantages: high value in latent heat, stable chemical properties, low cost, easy acquisition, no environmental pollution concerns, and compatibility with the materials used in air-conditioning equipment. However, there are a few disadvantages in using water as a PCM. Two of the most serious problems encountered are the supercooling

[1] Paper presented at the Fifteenth Symposium on Thermophysical Properties, June 22–27, 2003, Boulder, Colorado, U.S.A.

[2] Technological Research Laboratory in Energy, San Pablo Catholic University, Arequipa, Peru.
[3] Mechanical Engineering Department, Pontifical Catholic University of Rio de Janeiro. Rio de Janeiro. Brazil, CEP 22453-900.
[4] To whom correspondence should be addressed. E-mail: slbraga@mec.puc-rio.br

0195-928X/05/1100-1781/0 © 2005 Springer Science+Business Media, Inc.

phenomenon and the density inversion occurring in water solidification during the thermal storage cooling process.

When the water is cooled in an enclosed container, freezing does not occur at its freezing point (T_f) at atmospheric pressure. Instead, it is normally cooled below T_f before ice nucleation happens. Supercooled water refers to a state of metastable liquid even though the water temperature is below its freezing temperature. The metastable state ends when ice nucleation occurs and the thin plate-like crystals of dendritic ice grow into the supercooled region of water. During the dendritic ice growth process, latent heat is released from the dendritic ice and consumed by supercooled water. At the end of the growth process, the temperature of the water will return to its freezing point. If the metastable state exists and remains during the thermal storage process, thermal energy can only be stored in the form of sensible energy. In this case, the storage capacity is strongly reduced. Because of this, it is very important to prevent the occurrence of the supercooling and to acquire precise information from the water supercooling phenomenon during a thermal storage process.

There are several studies about the solidification of water: Gilpin [1] studied the dendritic ice formed inside a pipe during the freezing process. It has been shown that the growth of dendritic ice can cause blockage by the water inside the pipe. Chen and Lee [2] studied numerical and experimental methods to analyze the influence of nucleation agents in the water solidification process inside cylindrical copper capsules of different sizes. Tombari et al. [3] studied the variation of the supercooled water specific heat in a range of −30–10°C. Chen et al. [4] studied the supercooling phenomenon inside cylindrical capsules with and without nucleation agents. Yoon et al. [5] studied experimentally the freezing phenomenon of saturated water within the supercooled region in a horizontal circular cylinder using a holographic real-time interferometric technique. Okawa et al. [6] studied the freezing of supercooled water on a metallic plate. Milón and Braga [7] studied the phenomenon of supercooling in spherical capsules of different diameters and determined the parameters that influence the appearance of this phenomenon.

The present experimental study explores the supercooling phenomenon inside capsules of cylindrical geometry made from different materials. The objective of this paper is to understand this phenomenon and its advantages and disadvantages in the thermal storage process.

1.1. Supercooling in Capsules

According to Debenedetti [8], water can stay in a liquid state over a range of −41–280°C at atmospheric pressure. In Fig. 1 the freezing process

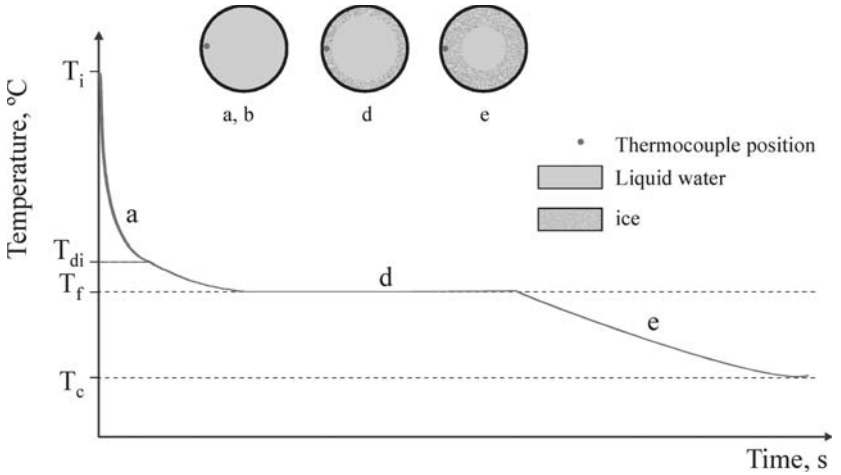

Fig. 1. Freezing process without supercooling, encapsulated water.

without supercooling is presented. This type of curve, with a stable phase change, normally happens in capsules of high thermal conductivity and low coolant temperatures (T_c). The process begins with the PCM temperature at T_i. This temperature drops while the liquid sensible heat is released (a). During this process the temperature passes through the density inversion temperature (T_{di}) and goes to the freezing temperature (T_f) where the latent heat is released (d) and the ice grows. The isothermal phase change process is evident. At the end of the solidification (region around the thermocouple), the sensible heat of the solid is released (e). In this process sequence, supercooling does not occur, dendritic ice does not appear, and the ice formation is crystalline.

In Fig. 2, the PCM is cooled, releasing sensible heat (a), to the density inversion temperature (T_{di}) and goes through the freezing temperature (T_f), and immediately afterwards, the temperature is reduced in the metastable liquid state (b) below T_f. The metastable state will end when ice nucleation occurs ($T = T_n$) and thin-plaque-like crystals of dendritic ice grow in the supercooled water region (c). During the dendritic ice growth process, latent heat is released from the dendritic ice and absorbed by the supercooled water. At the end of this dendritic growth process, the water temperature usually returns to its freezing point (T_f) and isothermal phase change starts (d). Later, the sensible heat of the solid is released (e). This behavior is common for different capsule materials for relatively low coolant temperatures.

In Fig. 3, a supercooling process with instantaneous freezing is shown. In this case, when nucleation occurs (c), the energy level is so low in this area that the PCM reaches T_f, and the phase change occurs quickly and immediately. After this, the release of sensible heat of the solid (e) starts. This process happens inside capsules with high thermal conductivity and low coolant temperatures.

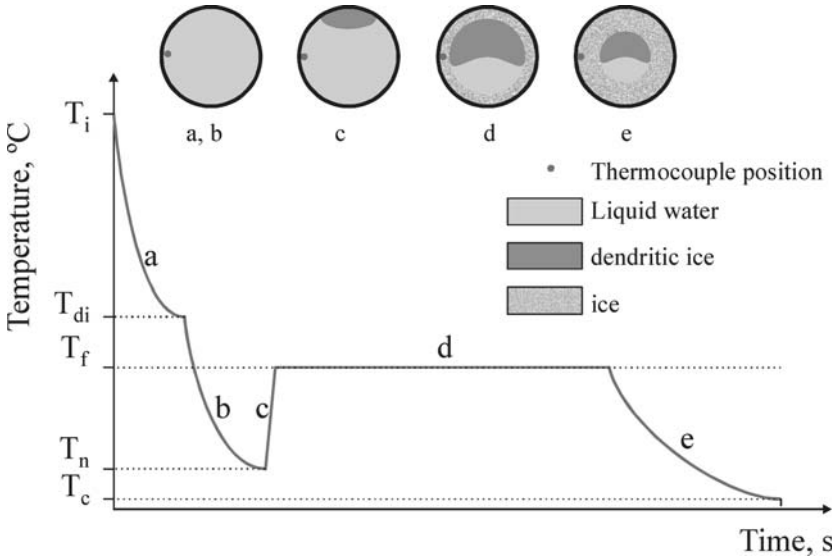

Fig. 2. Supercooling and freezing process, encapsulated water.

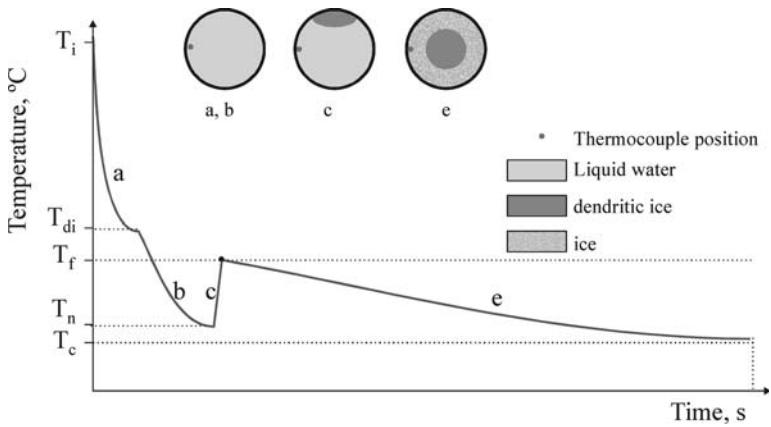

Fig. 3. Supercooling and instantaneous freezing process, encapsulated water.

In Fig. 4, the process of hypercooling with an instantaneous phase change is shown. Unlike the previous curve, the energy is still sufficiently low that, when nucleation occurs, the phase change occurs and the formed solid reaches a temperature below T_f (d) and immediately releases sensible heat (e).

In Fig. 5, the permanent supercooling and non-freezing process is observed. This occurs when the metastable liquid state (b) remains for an undetermined time and the PCM only releases liquid sensible heat. This curve is common in high- and low-thermal-conductivity capsules with high coolant temperatures (near T_f).

2. EXPERIMENTAL APPARATUS

The experimental apparatus, shown schematically in Fig. 6, consists of a test section (1), an observing system (2), a cooling system (3) and (4), and a measurement and data logging system (5).

2.1. Test Section

The test section contains the capsule under analysis. The walls are made of a 10 mm thick acrylic plate externally covered with 25 mm thick

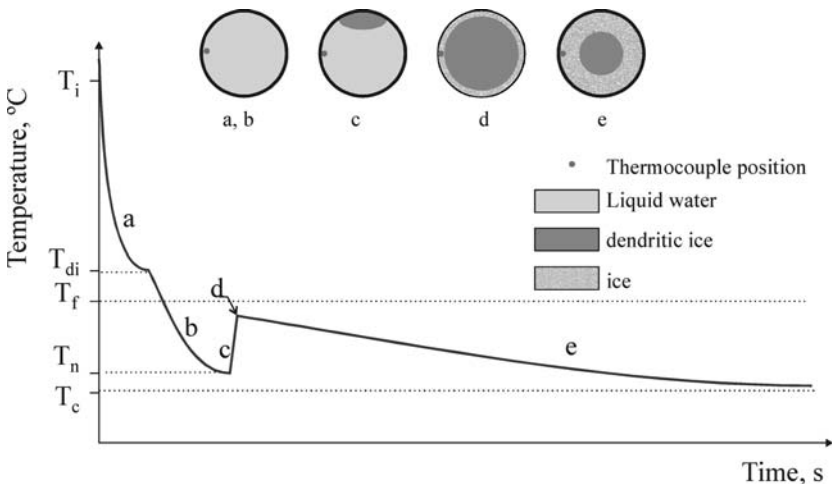

Fig. 4. Hypercooling and instantaneous freezing process, encapsulated water.

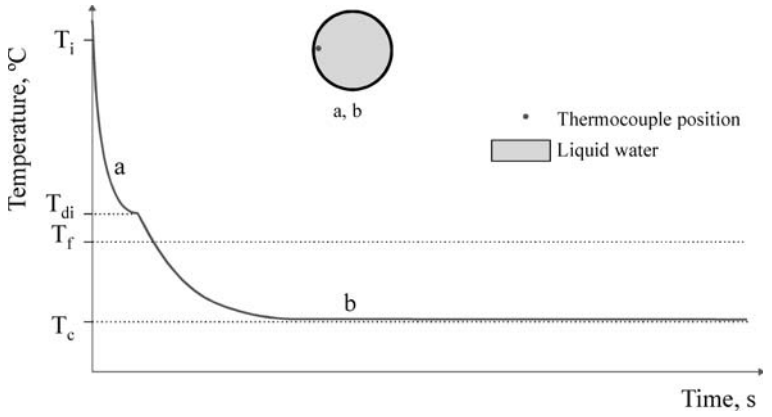

Fig. 5. Permanent supercooling and non-freezing process, encapsulated water.

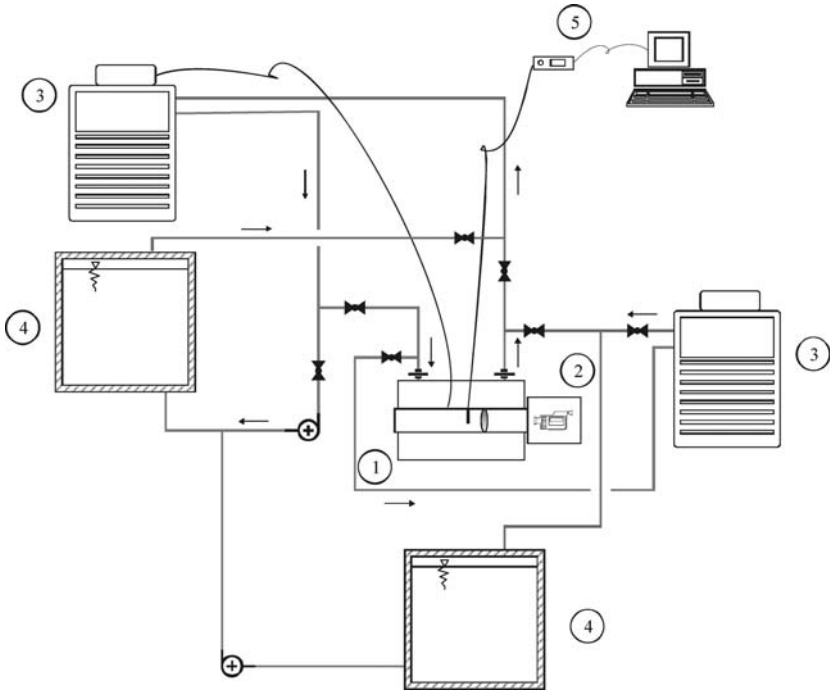

Fig. 6. Experimental apparatus schematic diagram: test section (1); observing section (2); cooling section: constant temperature bath (3), and reservoir (4, 5).

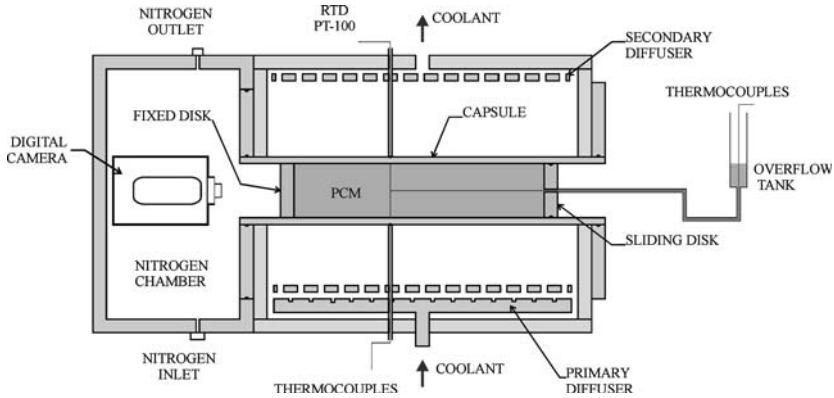

Fig. 7. Test section details.

insulation. A test section transversal cut is shown in Fig. 7. The diffuser is intended to homogenize the coolant temperature in the test section. The temperature control is carried out by a constant temperature bath which receives the signals from a temperature sensor – RTD type PT-100. K-type thermocouples were used for the circulating fluid temperature measurement. Two flanges are installed in the vertical walls to facilitate the cylinder change. An overflow tank, operating at atmospheric pressure, was installed to compensate the volume variation during the phase change. In the same figure, the cylindrical capsule, filled with the PCM, can be observed. K-type thermocouples of 0.076 mm diameter, covered with Teflon, are also indicated. Their positions are shown in Fig. 8 and reported in Table I. These thermocouples are used to determine the temperature during the experiments. To define the volume of the PCM, a sliding disk (movable in the axial direction) is used. The acrylic capsule is shown in Fig. 9. The PCM was distilled water to avoid contamination with external agents. Before placing the PCM inside the capsule; it was placed at rest, slightly warmed, to expel the dissolved air. The capsule was also carefully cleaned with distilled water. In the manufacturing process for the capsule, oil was not used in order to avoid contamination of the PCM.

2.2. Observing System

A digital camera (30 images per second), located inside a box, is used to register the exact instant of the nucleation and the growth of the ice. To avoid condensation, the space between the capsule and the camera lens is

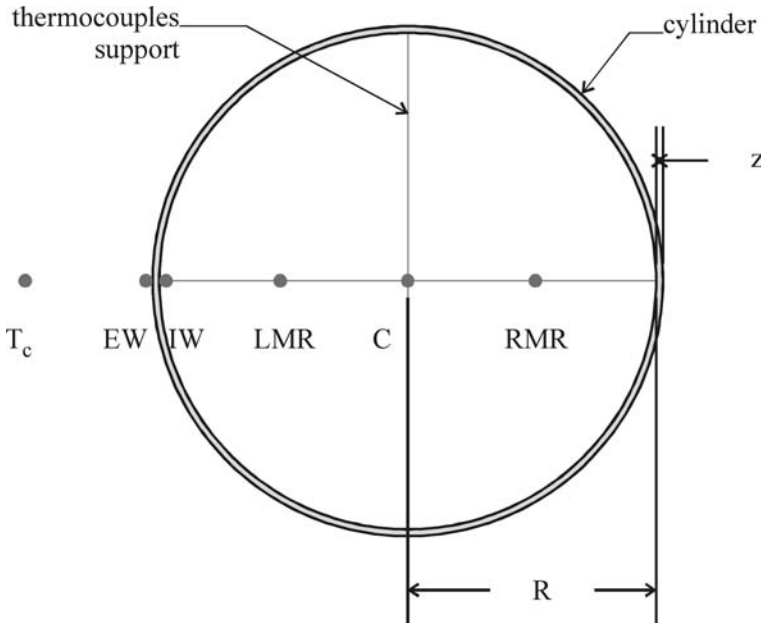

Fig. 8. Test cylinder view.

Table I. Temperature Sensors in the Capsule

Symbol	Description	Distance from the center line[a]
T_c	Coolant	$1.2R$
EW	External wall	$-(R+z)$
IW	Internal wall	$-R$
RMR	Right middle radius	$+R/2$
C	Center	0
LMR	Left middle radius	$-R/2$

[a] R is the cylinder radius, and z is the cylinder wall thickness.

filled with nitrogen, an inert gas that removes the humid air. The box is also insulated.

2.3. Cooling System

The cooling system can be seen in Fig. 6. It is composed of two constant temperature baths (CTB) (3), two reservoirs (4), and the coolant. The initial temperature for the tests is set for one CTB while the other

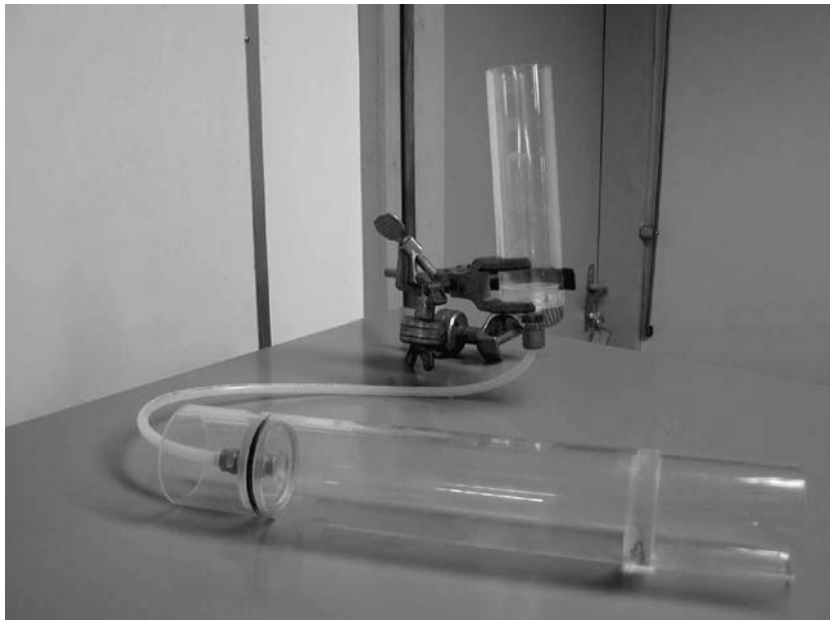

Fig. 9. Capsule front view with thermocouple distribution.

CTB is set at the test temperature. The temperature control system is of the PID type (proportional-integral-derivative), and it is able to maintain the temperature within a range of $\pm 0.05^{\circ}C$ with a refrigeration power of 800 W at $0^{\circ}C$ and 1000 W of electric power heater. The coolant is an alcohol–water solution (50% in volume).

2.4. Measuring and Data Logging System

The measurements and storage of data are carried out using an acquisition system and a personal computer (pc). The acquisition equipment, which communicates with the pc by an RS232 communication port, receives, processes, and transmits the temperature signals to the pc for storage and subsequent analysis.

3. EXPERIMENTAL PROCEDURE

The initial water temperature inside the capsule ($25^{\circ}C$) was imposed using a constant temperature bath (CTB). The cooling procedure starts by pumping the coolant through the upper reservoir while its temperature is

controlled by the second CTB. At this time the test section is empty at the initial temperature. When the desired test temperature is reached, the coolant is transferred to the test section absorbing the initial thermal loads and passed later to the underneath tank. When the upper tank is empty, the flow of the CTB is transferred toward the test section. After each test, a pump impels the coolant toward the upper reservoir for a new test. This procedure is carried out to maintain the test temperature constant for each test. A lapse of time shorter than 4 min is necessary for the coolant temperature to reach stability. This lapse represents less than 2.5% of the total test time. See Δt in Fig. 10.

The duration of each test varies from 1 to 5 h, depending on the test conditions and material of the capsule. If the nucleation does not happen within 5 h, the test is interrupted. The data are acquired once per second.

Uncertainties are presented in Table II based on the analysis presented by Moffat [9]. The critical experimental parameter was the temperature measurement. For this case the uncertainty was analyzed considering all components of the measuring and data logging system, thermocouples, etc.

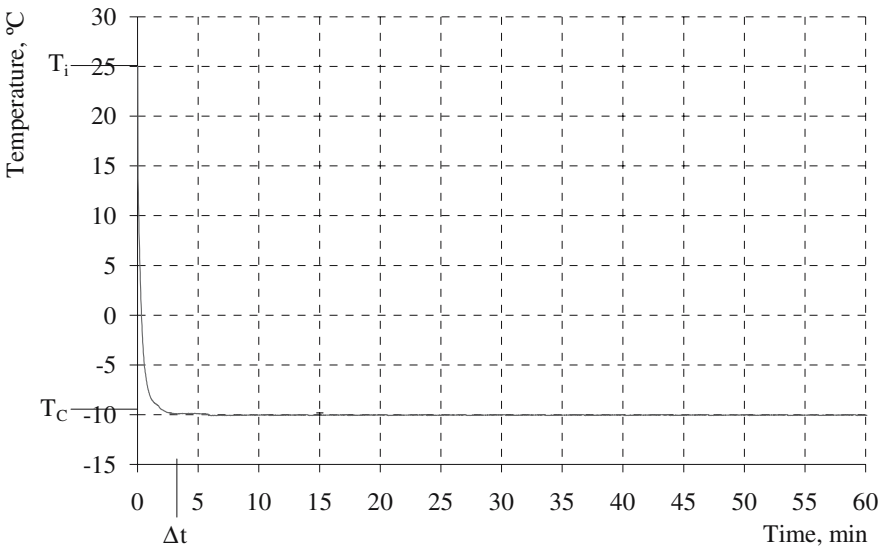

Fig. 10. Coolant temperature (T_c) during a typical test.

Table II. Uncertainties of Measurements

Parameter	Uncertainty
Temperature	0.1°C
Time	0.1 s
Length	0.1 mm

3.1. Investigated Parameters

The following parameters were investigated: supercooling and nucleation probability, cooling rate, and temperature field for cylindrical capsules made of acrylic, PVC, brass, and aluminum. All capsules have a 45 mm internal diameter and 1.5 mm wall thickness. Experiments were carried out for different coolant temperatures (T_c), varying from -2 to -10°C, in steps of 2°C. For each coolant temperature, the procedure was repeated 20 times, with the same initial and boundary conditions.

4. RESULTS AND DISCUSSION

4.1. Effect of the Cooling Rate

The cooling rate (CR) is defined as the relation between the inner wall average temperature variation evaluated from the start of supercooling until the nucleation and the completion of the supercooling, or,

$$\mathrm{CR} = \frac{\sum_{i=1}^{n} \mathrm{CR}_i}{n} = \frac{\sum_{i=1}^{n} \frac{\left(T_{\mathrm{IW}_i} - T_{\mathrm{IW}_{i-1}}\right)}{\Delta t'}}{n}, \quad \text{or} \quad \mathrm{CR} = \frac{\mathrm{SD}}{\Delta t} \tag{1}$$

where CR is the cooling rate in the internal wall; T_{IW_i} is the internal wall temperature; $\Delta t'$ is the time interval of acquisition data and n is the number of measurements; Δt is the total supercooling time, and SD is the supercooling degree.

Figure 11 shows a test for an acrylic capsule, $T_c = -6$°C, interrupted after 5 h of supercooling without nucleation. The effect of T_c can be observed in Figs. 12 and 13: brass, $T_c = -6$°C, $\mathrm{CR} = 0.082$°C$\cdot \mathrm{min}^{-1}$ and PVC, $T_c = -8$°C, $\mathrm{CR} = 0.214$°C$\cdot \mathrm{min}^{-1}$, respectively. In both cases, it is possible to observe the phenomenon of supercooling; but for larger T_c, the occurrence of nucleation takes longer. This behavior was always observed.

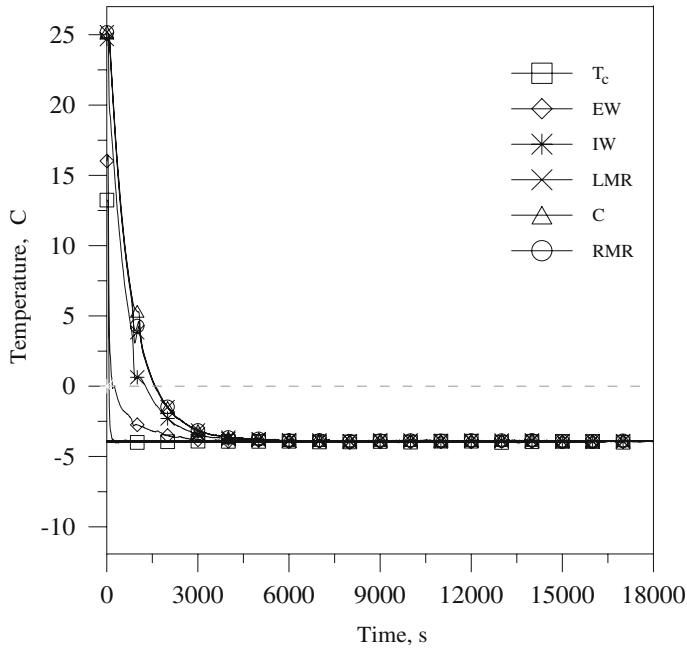

Fig. 11. Temperature versus time, acrylic, $T_c = -6°C$.

A solidification process without supercooling is observed in Fig. 14 for a brass capsule; $T_c = -8°C$, and the phase change occurs exactly at T_f. In Fig. 15, it is observed for the case of PVC, $T_c = -10°C$, $CR = 0.556°C \cdot min^{-1}$, the PCM starts supercooling (IW) and returns to T_f. It was caused, probably, by the convection due to the density inversion effect. After some time, the supercooling appears again and nucleation takes place, starting the solidification process. The IW temperature in Fig. 16 shows the aluminum capsule; $T_c = -10°C$, $CR = 0.609°C \cdot min^{-1}$, and hypercooling of the PCM (temperature in IW) is observed. When the nucleation occurs, the temperature rises to a value smaller then T_f and continues falling in the sensible stage.

Figure 17 shows the supercooling period as a function of cooling rate and material. It is possible to see the great influence of the CR. Large values of this variable imply short periods of supercooling.

According to the experiments, it was observed that the temperature of the internal wall of the capsule varies according to the position (upper, bottom, etc.). This could produce a consequence that the cooling rate also

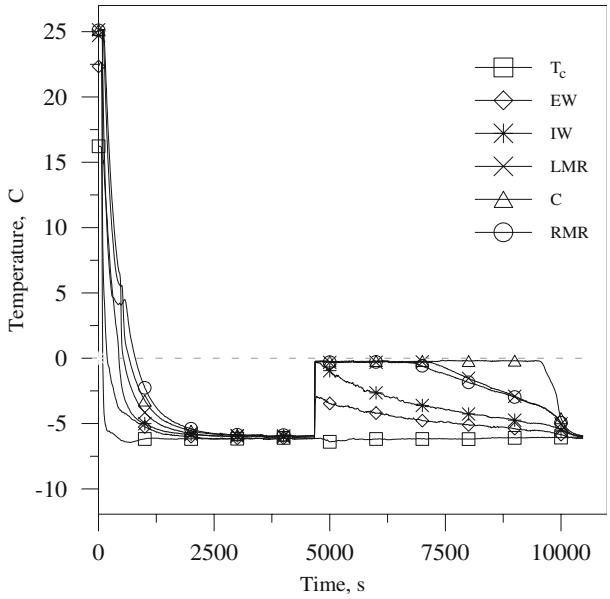

Fig. 12. Temperature versus time, brass, $T_c = -6°C$, $CR = 0.082°C \cdot min^{-1}$.

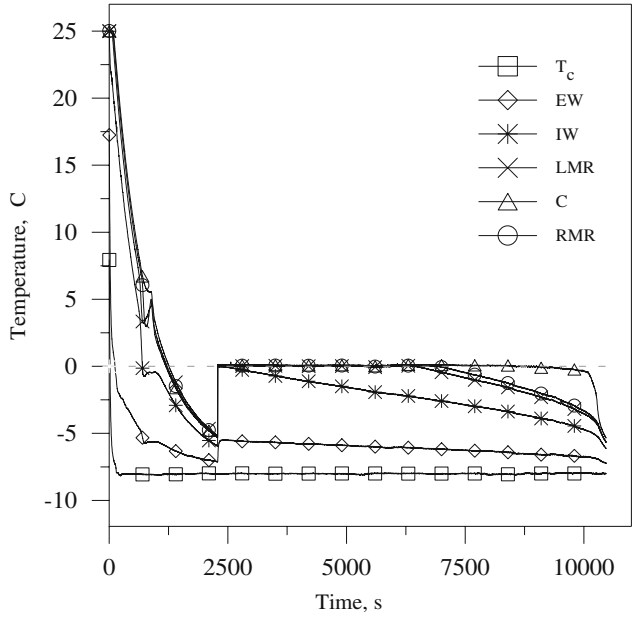

Fig. 13. Temperature versus time, PVC, $T_c = -8°C$, $CR = 0.214°C \cdot min^{-1}$.

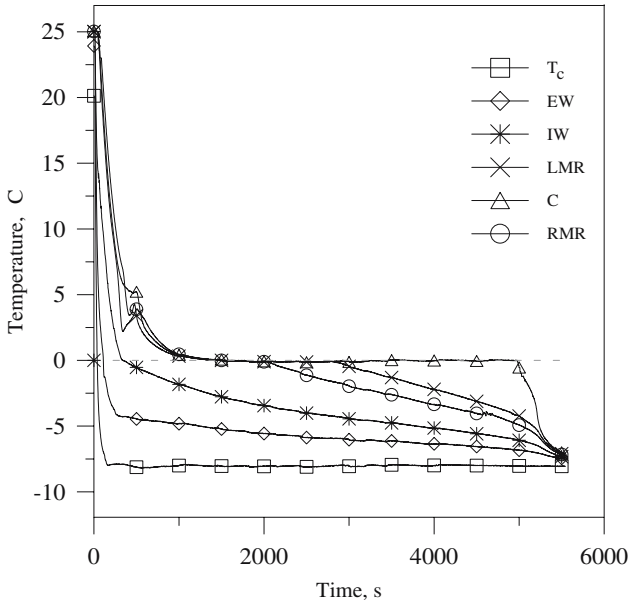

Fig. 14. Temperature versus time, brass, $T_c = -8°C$.

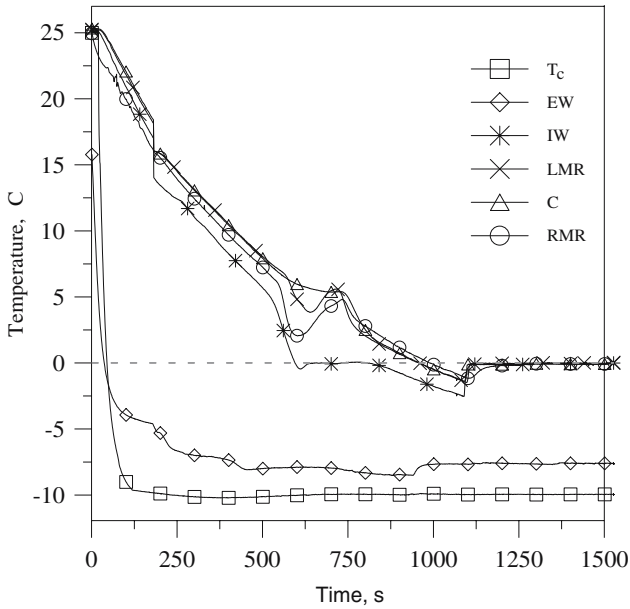

Fig. 15. Temperature versus time, PVC, $T_c = -10°C$, $CR = 0.556°C \cdot min^{-1}$.

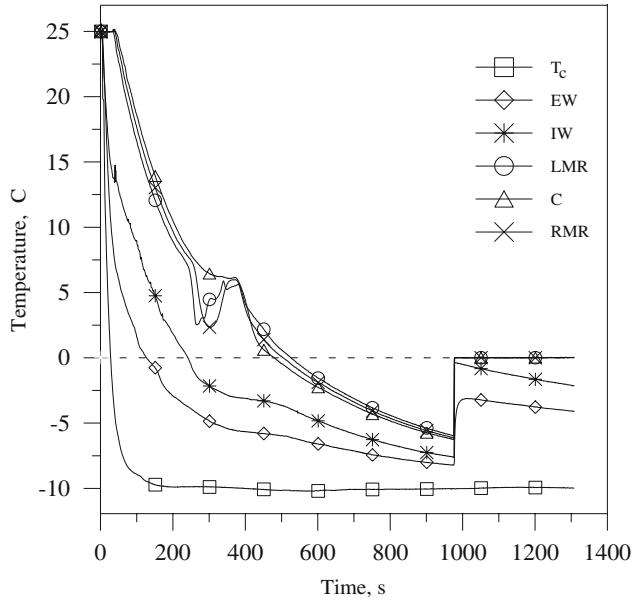

Fig. 16. Temperature versus time, aluminum, $T_c = -10°C$, $CR = 0.609°C \cdot min^{-1}$.

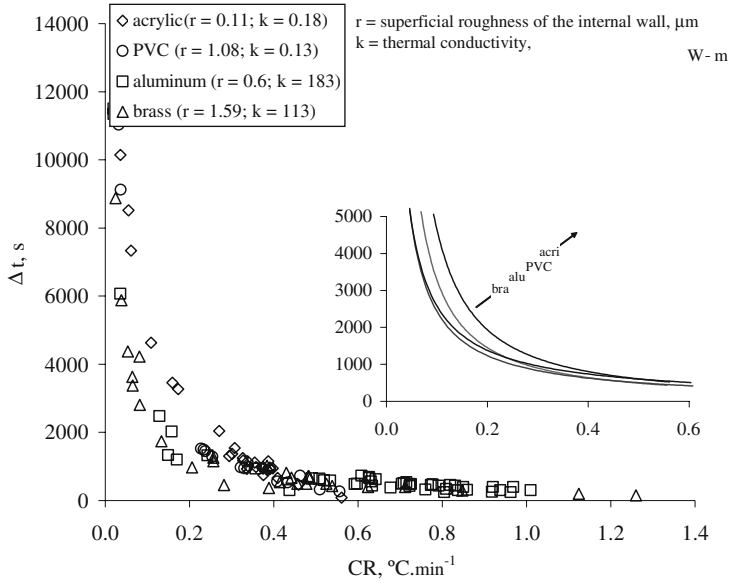

Fig. 17. Supercooling period as a function of the cooling rate, different materials.

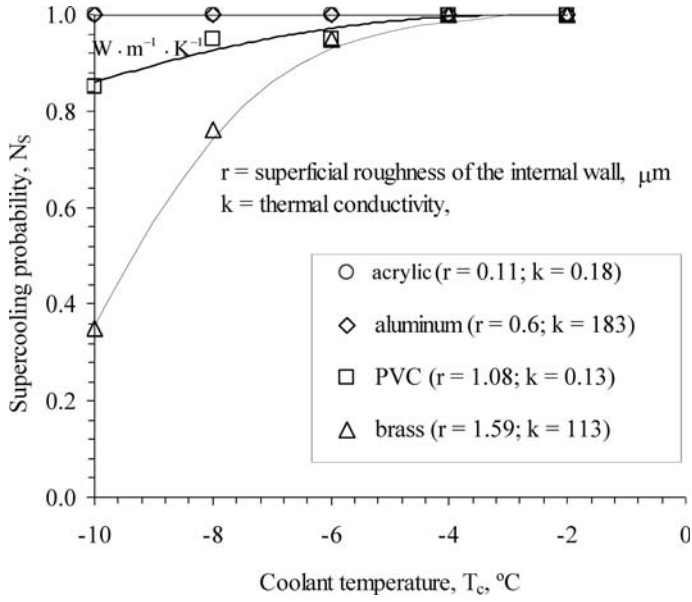

Fig. 18. Supercooling probability.

varies according to this position, and the reason for this behavior needs to be investigated further.

4.2. Effect of Coolant Temperature on Supercooling and Nucleation Probabilities

Figures 18 and 19 show the supercooling and nucleation probability, respectively, under different conditions of coolant temperatures, varying from -2 to -10°C for pure water, in the different capsules.

$$N_S = \frac{\text{number of observed supercoolings}}{\text{total number of tests}}, \quad N_F = \frac{\text{number of nucleations}}{\text{total number of tests}} \tag{2}$$

N_S and N_F are the supercooling and nucleation probabilities.

It is possible to see that the supercooling probability increases for larger T_c. For T_c of -2 and -4°C, this probability is 100%, independent of the material of the capsules. The acrylic capsules give a larger probability of supercooling, probably due to their low thermal conductivity. On the other hand, the aluminum capsule shows more cases of supercooling

then the PVC capsules. The reason for that could be its roughness and should be further investigated. The probability of nucleation is presented in Fig. 19 and shows that for high thermal conductivity materials, nucleation occurs more frequently. It can be explained by the stronger convection inside the capsules, facilitating the initiation of the freezing process.

In order to analyze the effect of the supercooling phenomenon, two materials of high thermal conductivity (aluminum and brass) and two materials of low thermal conductivity (acrylic and PVC) were used. In addition to the thermal conductivity of the capsule material, other factors (internal wall roughness, etc.) also affect this phenomenon.

4.3. Nucleation and Solidification Process

The nucleation process inside the acrylic capsule for $T_c = -8°C$ can be observed in Fig. 20. The left-hand side of the figure shows snapshots of the process captured during the test. On the right-hand side a schematic representation of the phenomenon is presented. The entire process takes about 3 s. In the first image the PCM is supercooled at $-8°C$ and, for this particular case, nucleation starts after 3500 s from the beginning of

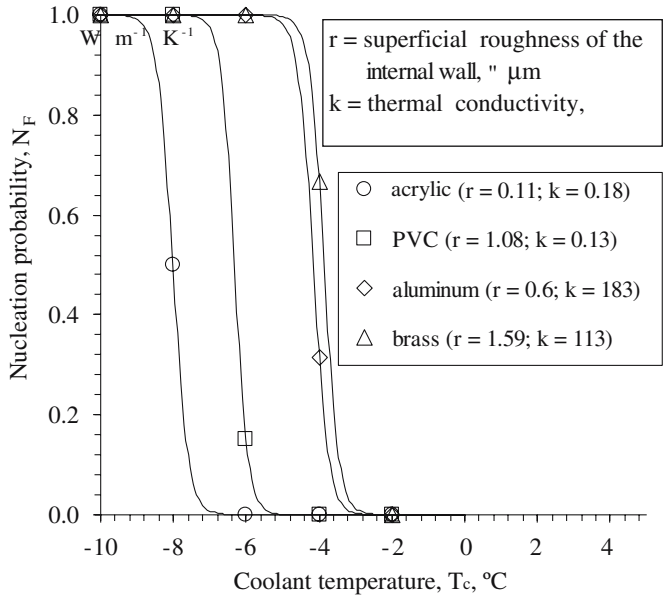

Fig. 19. Nucleation probability.

the cooling process. The sequence shows the development of scattered thin dendrites distributed inside the capsule. Figure 21 shows the continuation of the same case. After the nucleation, solid ice grows from the wall. This process is slower than for nucleation and takes approximately 4.6 h for completion. For each image of the sequence in Fig. 21, the corresponding instant of time is shown in minutes. Two different structures can be seen inside the capsule. A diffuse interface between the solid ice and the solid dendritic structure regions is observed. Figure 22 shows the images captured from the solidification process of the water without supercooling, for the aluminum capsule with $T_c = -6°C$. In this case the dendritic structure is not present and the interface is sharp and well defined. The total solidification process lasted 6.16 h.

5. CONCLUSION

The supercooling phenomenon was experimentally investigated inside cylindrical capsules filled with pure water, utilizing a phase change material (PCM) for cold storage systems. Cylinders with a 45 mm internal diameter and a 1.5 mm wall thickness, made from four different materials (acrylic, PVC, brass, and aluminum) were investigated. The water supercooling period and the nucleation temperature were investigated for different coolant temperatures. Characteristic curves of water cooling processes in cylindrical capsules with or without supercooling effects were observed. Particular experiments were done, where continuous metastable states were observed, or for cases of a double supercooling phenomenon. It was verified that the supercooling probability increases for larger T_c values. For T_c of -2 and $-4°C$, the probability of supercooling was 100%, independent of the material of the capsule. Nucleation occurs more frequently in experiments with high-thermal-conductivity materials. When supercooling occurs, dendritic ice accompanies the solidification process, along with the presence of a kind of mushy region. For the cases without supercooling, the interface between the ice and liquid water is well defined with no dendritic formation.

In summary, it is possible to observe that, to obtain a reliable thermal storage process, it should be advantageous to use capsules with high thermal conductivity and low values of T_c. The capsule material that presented less probability of supercooling was copper. Parameters such as internal wall roughness of the capsule should be further investigated.

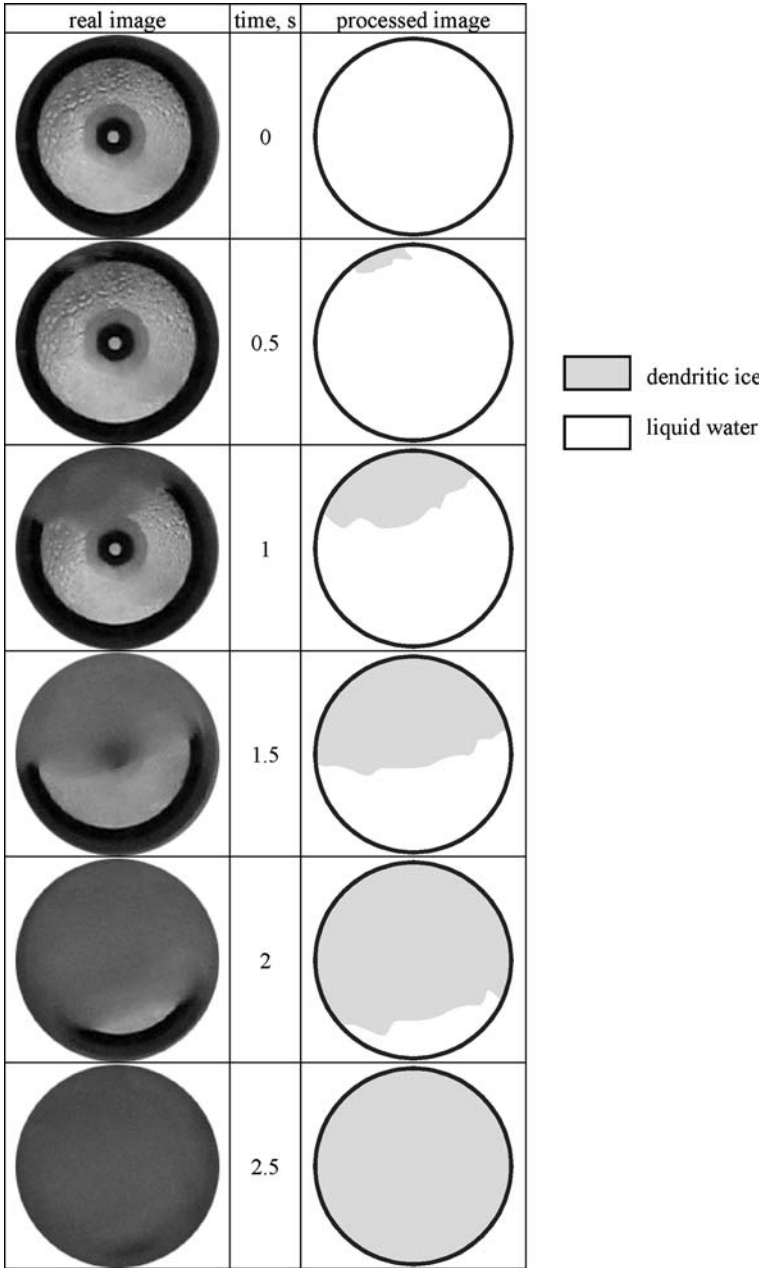

Fig. 20. Nucleation process: left column shows the real image, middle one shows the time (in s), and right one shows the processed image; acrylic with $T_c = -8°C$.

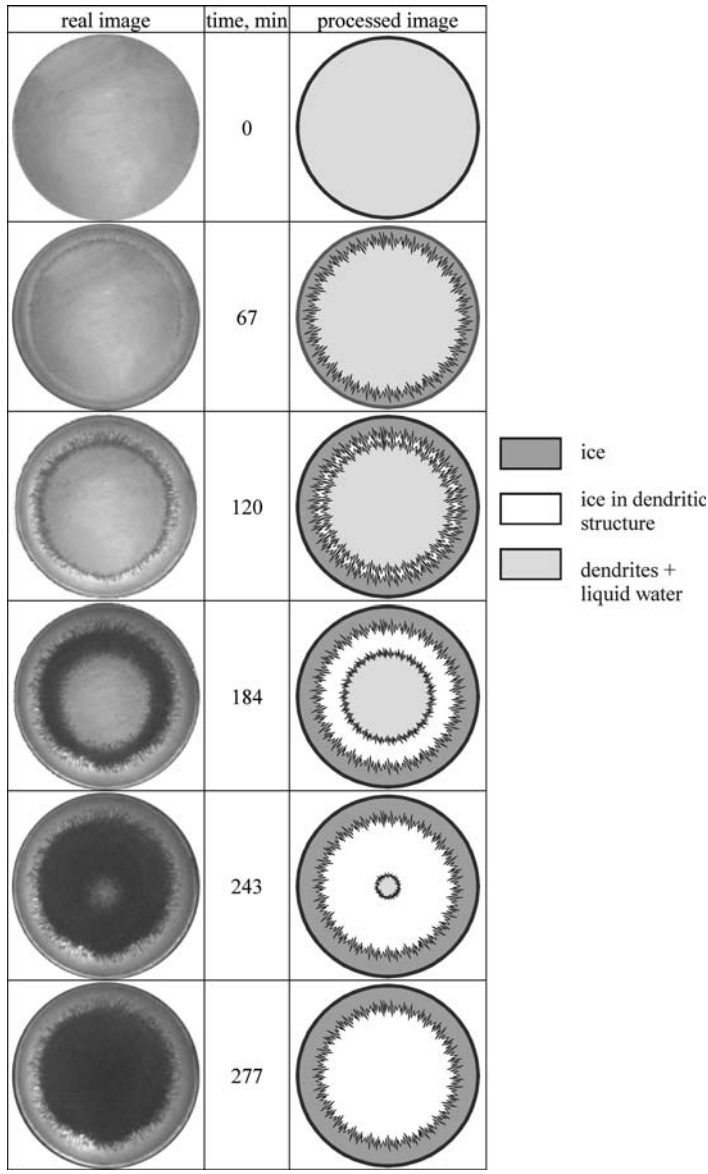

Fig. 21. Solidification process: left column shows the real image, middle one shows the time (in min), and right one shows the processed image. acrylic with $T_c = -8°C$.

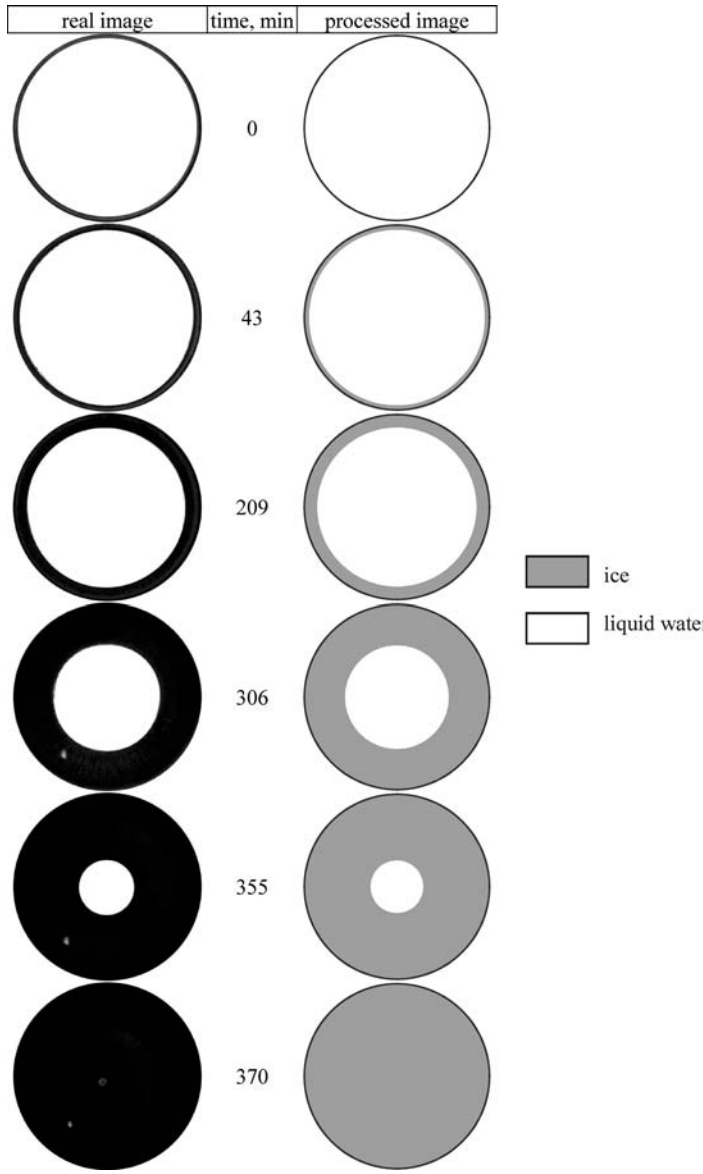

Fig. 22. Solidification process: left column shows the real image, middle one shows the time (in min), and right one shows the processed image; brass with $T_c = -6^\circ C$.

NOMENCLATURE

T	temperature, °C
T_c	coolant temperature, °C
T_{di}	density inversion temperature, °C
T_i	initial temperature, °C
T_f	phase change temperature, °C
T_n	nucleation temperature, °C
SD	supercooling degree, °C
N_S	supercooling probability
N_F	nucleation probability
CR	cooling rate, $°C \cdot min^{-1}$

Convention

PCM	phase change material
Δt	duration of the supercooled state
CTB	constant temperature bath
PVC	polyvinyl chloride
PID	proportional, integral, and derivative control

REFERENCES

1. R. R. Gilpin, *ASME J. Heat Transfer* **99**:419 (1977).
2. S. L. Chen and T. Z. Lee, *Int. J. Heat Mass Transfer* **41**:769 (1998).
3. E. Tombari, C. Ferrari, and G. Salvetti, *Chem. Phys. Lett.* **300**:749 (1999).
4. S. Chen, P. Wang, and T. Lee, *Exp. Therm. Fluid Sci.* **8**:299 (1999).
5. J. I. Yoon, C. G. Moon, E. Kim, Y. S. Son, J. D. Kim, and T. Kato, *Appl. Therm. Eng.* **21**:657 (2001).
6. S. Okawa, A. Saito, and R. Minami, *Int. J. Refrig.* **24**:108 (2001).
7. J. J. Milón and S. L. Braga, presented at 4th Eur. Therm. Sci. Conf., Birmingham, United Kingdom (2004).
8. P. Debenedetti, *Metastable Liquids, Concepts and Principles* (Princeton University Press, Princeton, New Jersey, 1996).
9. R. J. Moffat, *J. Fluids Eng.* **107**:173 (1985).